A Comparative Study of Linear vs. Nonlinear Data-Driven Modeling Accuracy and Fault Detection Sensitivity in Chemical Processes

Nour Basha[1], Byanne Malluhi[2], Hazem Nounou[1], and Mohamed Nounou[1,*]

***Abstract*— Data-driven process monitoring frameworks depend on the quality of the underlying model to accurately represent normal operating behavior, as modeling errors propagate directly into fault detection residuals. In this paper, a two-stage comparative analysis is presented of three data-driven modeling approaches: Principal Component Analysis (PCA), Bayesian-Optimized Kernel PCA (BOKPCA), and Bayesian-Optimized Neural Networks (BONN). First, their prediction accuracy is evaluated at different noise levels and reduced dimensionalities, and then assessing how this accuracy translates into fault detection performance. Modeling accuracy is quantified using the mean squared error (MSE) relative to noise-free data across a range of signal-to-noise ratios. Fault detection performance is subsequently evaluated using the Maximum Multivariate Generalized Likelihood Ratio chart, augmented through interval data analysis. Three case studies are used: a nonlinear synthetic dataset, the Tennessee Eastman Process, and a bench-scale Fischer-Tropsch Gas-to-Liquid reactor. The modeling results show that BONN consistently achieves a lower MSE than PCA across noise levels, while BOKPCA's model selection accuracy degrades at higher noise. These trends carry through to fault detection, where BONN's modeling advantage translates into higher detection rates, particularly for mean-shift and slow-drift fault types in processes with strong nonlinear dynamics and limited training data.**

I. INTRODUCTION

Equipment failure and other process faults are estimated to cost upward of 50 billion dollars per year globally in the chemical industry. In response, significant resources have been directed toward the development of data-driven process monitoring (PM) frameworks capable of characterizing normal operating behavior and flagging deviations from it using process data alone, without requiring explicit first-principles models. Such frameworks are particularly valuable for complex, high-dimensional chemical processes where mechanistic models are difficult or costly to derive. A complete data-driven PM framework consists of three sequential stages: modeling, fault detection (FD), and fault classification. In the modeling stage, a baseline representation of fault-free process behavior is constructed. During fault detection, deviations of incoming process data from this baseline are flagged using statistical charts. Finally, fault classification identifies the physical source of the detected anomaly [1].

Modeling is the foundation upon which both subsequent stages depend, where a poor model produces unreliable residuals, and even the most sophisticated detection chart cannot compensate for a fundamentally inaccurate representation of the process. Despite its foundational role, the modeling stage is rarely the primary focus of comparative process monitoring studies. Most published work evaluates competing methods solely on fault detection or classification metrics, without explicitly quantifying how differences in modeling accuracy relate to differences in downstream performance. This creates a gap in understanding: when one model outperforms another in fault detection, it is unclear whether the advantage stems from superior modeling accuracy, better noise suppression, or the particular fault type being tested.

Principal Component Analysis (PCA) is a widely used modeling technique for data-driven fault detection, owing to its computational simplicity and well-understood theoretical properties [2], [3]. For processes with linear dynamics and well-separated fault signatures, PCA provides a reliable baseline. However, real industrial processes frequently exhibit significant nonlinearities, and PCA's linear decomposition can fail to capture these dynamics accurately, leading to higher residuals under normal operating conditions and degraded detection sensitivity. Two nonlinear alternatives to PCA have been developed in recent work: Kernel PCA (KPCA), which maps data to a higher-dimensional feature space to linearize nonlinear relationships [4], and neural network-based auto-encoders, which learn nonlinear mappings through Bayesian-optimized deep structures [5]. Both approaches have been combined with Bayesian optimization (BO) to automate hyperparameter selection, yielding the BOKPCA and BONN frameworks respectively.

This paper examines the modeling accuracies and fault detection performances of the aforementioned methods using the following case studies: a synthetic nonlinear model, the Tennessee Eastman Process (TEP), and a bench-scale Fischer-Tropsch GTL reactor. First, the modeling accuracies of PCA, BOKPCA, and BONN are benchmarked using the mean squared error (MSE) relative to noise-free data across a range of signal-to-noise ratios (SNR) and reduced dimensionalities. Second, this paper evaluates how these differences in modeling accuracy propagate into fault detection performance using the Maximum Multivariate Generalized Likelihood Ratio (MMGLR) chart [6], [7] and interval data analysis.

While the individual methods and datasets have been studied in prior work [1], [6], [7], [5], the explicit two-stage analysis linking modeling accuracy directly to fault detection sensitivity within a unified comparative framework has not been presented. This paper fills that gap, and is organized as follows. Section II introduces the modeling frameworks,

[1] College of Science and Engineering, Hamad Bin Khalifa University, Doha, Qatar

[2] Department of Chemical Engineering, Texas A&M University, College Station, TX, USA

[*] Corresponding author: mnounou@hbku.edu.qa

detection charts, and interval data analysis methods used. Section III presents and interprets the comparative results across all three case studies. Section IV summarizes the key findings and their implications for model selection in practice.

II. METHODOLOGY

A. Modeling: Principal Component Analysis (PCA)

PCA is a linear dimensionality reduction technique that constructs an orthogonal basis via eigendecomposition of the variable correlation matrix. A reduced set of $r < p$ principal components is retained, yielding a low-rank reconstruction $\hat{X}$; the residuals $\tilde{X} = X - \hat{X}$ serve as input to the fault detection stage. The reduced dimensionality r is selected via scree plots [5].

B. Modeling: Bayesian-Optimized Kernel PCA (BOKPCA)

Kernel PCA extends PCA to nonlinear data by implicitly mapping inputs to a high-dimensional feature space via a kernel function (e.g., the Gaussian RBF kernel), avoiding explicit computation of the mapping. PCA is applied to the resulting kernel matrix, and predictions in the original input space are recovered via a pre-image estimation step using kernel density estimation [4]. Bayesian optimization (BO) selects the forward and reverse kernel types and their hyperparameters by minimizing cross-validation MSE in the feature space.

C. Modeling: Bayesian-Optimized Neural Networks (BONN)

BONN is a nonlinear auto-encoder whose input and output layers both represent the p process variables; a bottleneck hidden layer of dimensionality r forces a compressed representation analogous to PCA's retained components. The structural hyperparameters (depth, layer widths, activation functions) are selected via BO using cross-validation MSE, while weights and biases are optimized via conjugate gradient descent with backpropagation [5].

D. Modeling: Performance Assessment

When noise-free data $\bar{X}$ is available (i.e., synthetic case study), accuracy is quantified by the MSE between the model prediction $\hat{X}$ and $\bar{X}$, evaluated across a range of r and SNR values. When ground truth is unavailable (i.e., real data case study), dimensionality r is selected via scree plots for the PCA and BONN models, or via the elbow of the cross-validation MSE curve in feature space for the BOKPCA model [4], and accuracy is assessed visually through prediction plots: a more accurate model produces smoother predictions that suppress noise without distorting process dynamics [1].

E. Fault Detection: Q Chart

The Q chart, also known as the squared prediction error (SPE) chart, is the simplest and most widely used fault detection chart. For a given test sample $s[i]$, its Q statistic is computed from the model residuals $\tilde{s}[i]$ as follows:

$$\Omega[i] = \frac{1}{p}\sum_{k=1}^{p} \tilde{s}_k[i]^2. \tag{1}$$

A threshold γ is computed from the empirical cumulative distribution of the training statistics at a predefined confidence level α, and a sample is declared faulty if its statistic exceeds this threshold.

F. Fault Detection: Maximum Multivariate Generalized Likelihood Ratio (MMGLR) Chart

The Generalized Likelihood Ratio (GLR) chart is a hypothesis-testing chart that quantifies the probability that a given residual belongs to the fault-free distribution [8], [9]. For each univariate residual signal and a moving window size β_{GLR}, the GLR statistic for changes in mean is defined as follows:

$$\omega_j[i] = \max_{k\in[0,\,\beta_{\text{GLR}}-1]} \frac{k+1}{2\sigma_0^2}\left(\mu_{(1,k,i)} - \mu_0\right)^2, \tag{2}$$

where μ_0 and σ_0^2 are the training mean and variance of variable j, and $\mu_{(1,k,i)}$ is the sample mean over the moving window ending at sample i.

To extend the univariate GLR chart to multivariate residuals, the MMGLR chart takes the maximum statistic across all p variables at each sample, such that $\Omega[i] = \max_{1\le j\le p} \omega_j[i]$. This aggregation strategy controls false alarm rates more effectively than the conventional multivariate GLR (MGLR) formulation, which raises a fault flag whenever *any* variable crosses its individual threshold. The threshold for the MMGLR chart is set as $\gamma = c_\alpha \cdot \gamma_{95\%}$, where $\gamma_{95\%}$ is the threshold computed at $\alpha = 95\%$ and c_α is an unbounded multiplier that provides finer control over the chart's accuracy [7].

G. Fault Detection: Interval Data

Interval data representation augments scalar process measurements with local variability information through Moving Window Interval Aggregation (MWIA). For a scalar signal x and a window of size β, the interval center $c[i]$ and radius $r[i]$ are computed as the window mean and standard deviation respectively, defining the interval $[c[i]-r[i],\ c[i]+r[i]]$. Centers are more sensitive to changes in the process mean, while radii better capture changes in process variance. As a result, models are built separately on centers and radii, and their detection vectors are combined via a logical OR gate, so that a sample is declared faulty if either chart raises an alarm [10], [6]. The window size β is an optimizable hyperparameter selected to balance detection sensitivity against the inertial shift introduced by moving window aggregation [11].

H. Fault Detection: Performance Metrics

Performance is quantified via ROC curves (detection rate DR vs. false alarm rate FAR). Detection rates at FAR $\approx 1\%$ are reported, and an optimized metric $\hat{e}$ is computed as the minimum Euclidean distance from the ROC curve to the ideal

point (FAR $= 0\%$, DR $= 100\%$), with FAR constrained to $\leq 10\%$. A smaller $\hat{e}$ indicates better performance [1].

III. RESULTS AND DISCUSSION

A. Modeling Accuracy

1) Synthetic Nonlinear Model: The synthetic dataset is defined by ten variables with nonlinear interdependencies governed by combinations of sinusoidal, polynomial, exponential, and tangent functions of two underlying frequency-modulated signals; full details of the data generator are provided in [1]. A Monte Carlo simulation of 100 realizations is used, with 1000 training and 1000 testing samples per realization. Modeling accuracy is evaluated across SNR $\in \{5, 50\}$, representing high and low noise conditions respectively. For PCA and BONN, a scree plot estimates the optimal dimensionality as $\hat{r} = 4$ at both SNR values, which is a reasonable approximation to the true optimal values of $r^* = 4$ for PCA and $r^* = 3$ for BONN. The optimal BONN model structures selected via Bayesian optimization using 5-fold cross-validation are: scalar $m = [10, 4, 16, 20, 10]$, $\Psi = \{\text{linr, linr, LRLU, tanh, linr}\}$; interval centers $m = [10, 4, 19, 10]$, $\Psi = \{\text{linr, linr, LRLU, linr}\}$; interval radii $m = [10, 7, 5, 10]$, $\Psi = \{\text{linr, linr, linr, linr}\}$. The corresponding MSE values are reported in Table I.

For BOKPCA, the optimal dimensionalities are estimated from the cross-validation MSE plot in the feature space as $\hat{r} = [10, 5, 10]$ for scalar, interval center, and interval radii data respectively (at SNR $= 10$, used for fault detection). The selected BOKPCA models are: (1) scalar ($r = 10$): Sigmoid forward kernel, Polynomial reverse kernel, $\eta = 0.0075$; (2) interval centers ($r = 5$): Polynomial forward kernel, Polynomial reverse kernel, $\eta = 0.0013$; (3) interval radii ($r = 10$): Sigmoid forward kernel, Laplacian reverse kernel, $\eta = 0.0011$ [1], [7].

At SNR $= 5$, BONN achieves the lowest MSE of 0.056 at $r = 3$, outperforming PCA (0.074 at $r = 4$) and BOKPCA (0.082 at $r = 5$). At SNR $= 50$, BONN and BOKPCA reach equivalent minima of 0.008, both substantially below PCA (0.017 at $r = 4$). The estimated optimal dimensionality for BOKPCA degrades at high noise ($\hat{r} = 11$ at SNR $= 5$ vs. true $r^* = 5$), reflecting the greater sensitivity of the feature-space model selection criterion to noise compared to scree-plot-based selection [1]. Figure 1 visualizes these curves across all dimensionalities for both noise levels.

2) Tennessee Eastman Process (TEP): The TEP dataset consists of 52 process variables. For PCA and BONN, a scree plot selects $r = 32$ for scalar data, $r = 26$ for interval centers, and $r = 37$ for interval radii. The selected BONN models are: scalar $m = [52, 32, 65, 52]$, $\Psi = \{\text{linr, linr, LRLU, linr}\}$; interval centers $m = [52, 26, 52]$, $\Psi = \{\text{linr, linr, linr}\}$; interval radii $m = [52, 37, 52]$, $\Psi = \{\text{linr, sigm, linr}\}$. For BOKPCA, the cross-validation MSE plot in the feature space selects an optimal dimensionality of $r = 40$, with a Polynomial forward kernel ($c_1 = 0.0011$, $c_2 = 4.973$, $c_3 = 2$), a Gaussian reverse kernel ($\sigma_f = 1$, $1/\sigma_l^2 = 0.3203$), and regularization parameter $\eta = 0.0282$ [1].

TABLE I: MSE of PCA, BONN, and BOKPCA models relative to noise-free testing data, averaged over 100 Monte Carlo realizations. Bold denotes optimal r per model per SNR.

r	PCA		BONN		BOKPCA	
	SNR=5	SNR=50	SNR=5	SNR=50	SNR=5	SNR=50
2	0.154	0.146	0.096	0.083	0.175	0.127
3	0.074	0.034	**0.056**	**0.008**	0.091	0.011
4	**0.074**	**0.017**	0.073	0.009	0.090	**0.008**
5	0.084	0.011	0.087	0.011	**0.082**	0.008
6	—	—	—	—	0.104	0.010
7	—	—	—	—	0.130	0.014
8	—	—	—	—	0.134	0.014

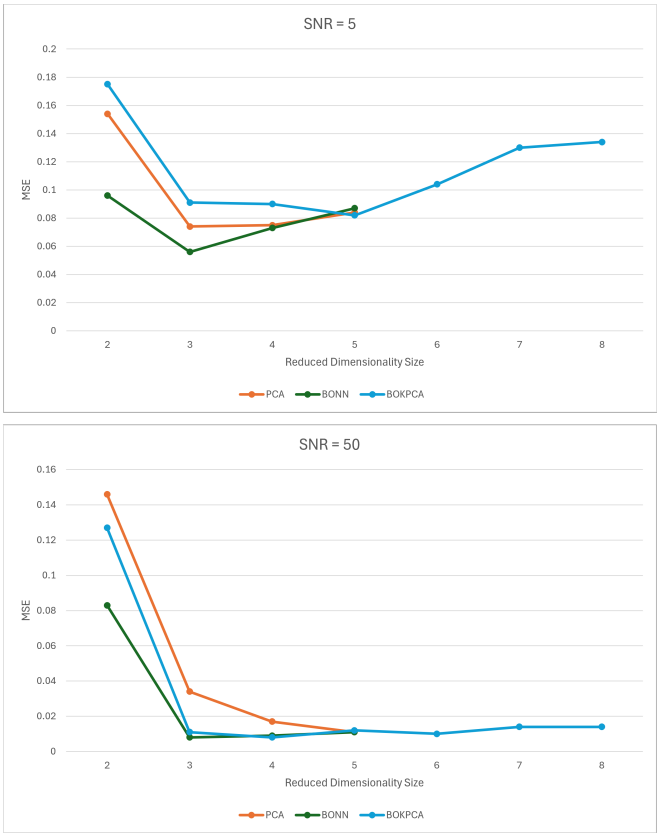

Fig. 1: Synthetic data: MSE of PCA, BONN, and BOKPCA at different reduced dimensionalities r, for SNR = 5 (top) and SNR = 50 (bottom) [1].

Figures 2 and 3 compare the prediction accuracies of the BONN and PCA models for TEP Variables 13 and 18 respectively. Figure 4 shows the prediction accuracy of the BOKPCA model for the same variables. Since the TEP dataset has a relatively high amount of noise compared to what is expected from typical industrial data, all three models exhibit similar levels of robustness and their predictions are almost identical. This observation is consistent with the synthetic case study: when noise dominates the signal, the

advantage of nonlinear modeling is diminished, as all models are primarily fitting noise rather than process dynamics. The prediction plots do not reveal a meaningful difference between PCA, BONN, and BOKPCA for the TEP, and this result directly foreshadows the near-equivalent fault detection performance observed in Section III-B [1].

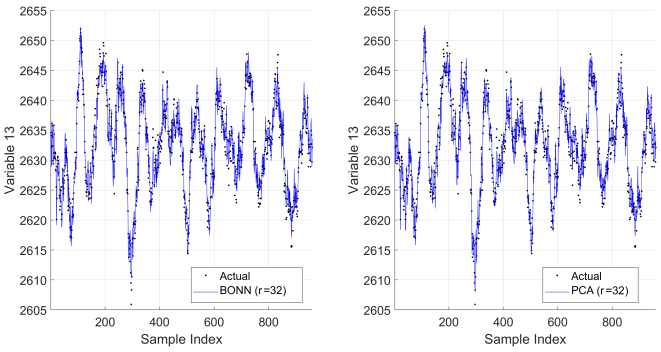

Fig. 2: TEP: model predictions of BONN (left) and PCA (right) for Variable 13 at $r = 32$. Both models produce nearly identical predictions due to the high noise level in the TEP dataset [1].

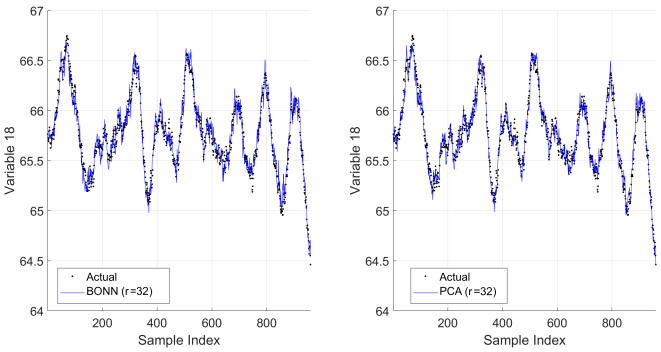

Fig. 3: TEP: model predictions of BONN (left) and PCA (right) for Variable 18 at $r = 32$. As with Variable 13, predictions are visually indistinguishable between models [1].

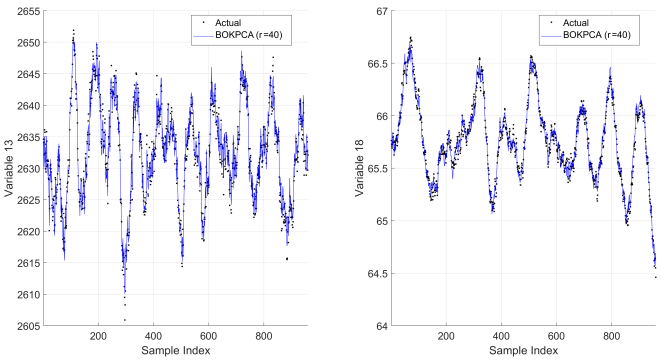

Fig. 4: TEP: model predictions of BOKPCA for Variables 13 (left) and 18 (right) at $r = 40$. BOKPCA's predictions are similarly close to the actual data, confirming that all three models perform comparably on the TEP [1].

3) Bench-Scale Fischer–Tropsch GTL Reactor: The GTL dataset consists of 18 measured variables sampled at 15-minute intervals. For PCA and BONN, a scree plot selects $r = 10$ for all data types. The selected BONN models are: scalar $m = [18, 10, 33, 18]$, $\Psi = \{\text{linr, linr, LRLU, linr}\}$; interval centers $m = [18, 10, 35, 18]$, $\Psi = \{\text{sigm, linr, sigm, linr}\}$; interval radii $m = [18, 10, 35, 18]$, $\Psi = \{\text{linr, linr, LRLU, linr}\}$. For BOKPCA, the cross-validation MSE plot in the feature space selects an optimal dimensionality of $r = 18$, with a Polynomial forward kernel ($c_1 = 0.0052$, $c_2 = 4.0802$, $c_3 = 1$), a Laplacian reverse kernel ($1/c_1 = 0.0851$), and regularization parameter $\eta = 0.0011$ [1].

Figures 5 and 6 compare the prediction accuracies of BONN and PCA for GTL variables LIC-1 and TI-1 respectively. In contrast to the TEP, a clear difference emerges between the linear and nonlinear models. BONN tracks the actual measurements tightly across both steady-state and transient operating regions, while PCA exhibits clear divergence and spurious oscillations — most visibly in the nonlinear transition region around samples 130–200 in Figure 6, where the reactor temperature ramps nonlinearly. Figure 7 shows BOKPCA predictions for variables 02 and 09, which are also closely aligned with the measured data. The lower number of random fluctuations in both nonlinear models' predictions indicates a higher robustness to measurement noise compared to PCA, confirming that the BOKPCA and BONN models better capture the dynamics of the GTL data [1]. This qualitative modeling advantage directly foreshadows the large fault detection performance gap between BONN and PCA observed in the GTL case study.

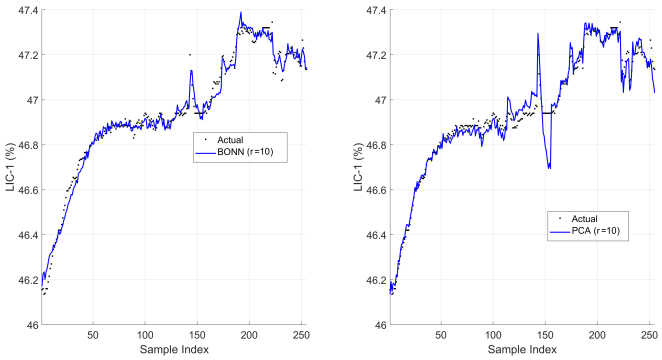

Fig. 5: GTL process: model predictions of BONN (left) and PCA (right) for LIC-1 at $r = 10$. BONN tracks the actual data closely while PCA introduces spurious fluctuations [1].

B. Fault Detection

Full per-fault detection rate and $\hat{e}$ tables for all case studies are already reported in previous work [7], [1]. All three models (i.e., PCA, BOKPCA, and BONN) are evaluated on the synthetic dataset. For the TEP and GTL case studies, only PCA and BONN are carried forward. This decision follows directly from Section III-A: BOKPCA's feature-space model selection substantially overestimated the optimal

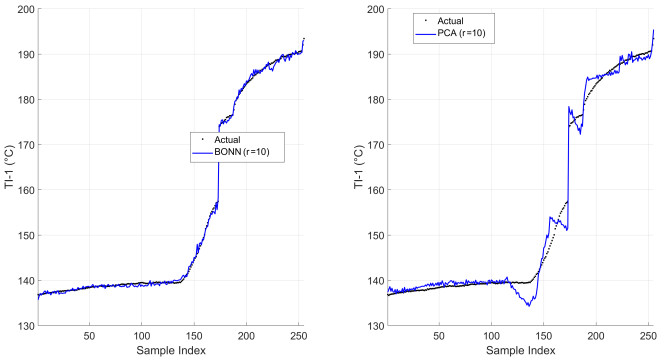

Fig. 6: GTL process: model predictions of BONN (left) and PCA (right) for TI-1 at $r = 10$. PCA diverges significantly from the actual data through the nonlinear transition region (samples 130–200) [1].

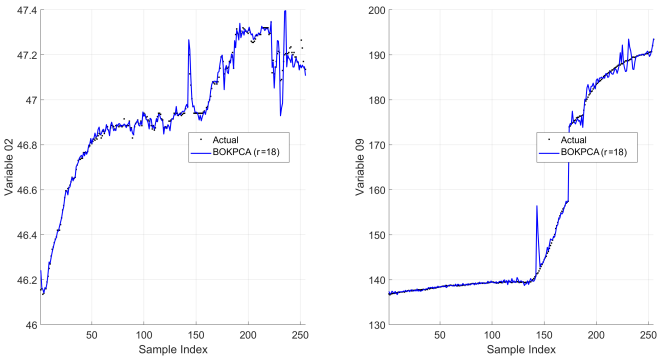

Fig. 7: GTL process: model predictions of BOKPCA for variables 02 (left) and 09 (right) at $r = 18$. Close agreement with measured data confirms the superior noise suppression of nonlinear models relative to PCA [1].

dimensionality under high noise ($\hat{r} = 11$ vs. $r^* = 5$), making its residuals unreliable in settings where ground-truth MSE is unavailable to verify selection accuracy. Table II summarizes the average $\hat{e}$ values using the best-performing combination (MMGLR chart with interval data) for PCA and BONN across all three case studies, together with the BOKPCA result for the synthetic case.

In the synthetic case study, the detection ranking (i.e., BONN ($\hat{e} = 25.8$) $>$ BOKPCA ($\hat{e} = 27.9$) $>$ PCA ($\hat{e} = 31.6$)) is directly consistent with the MSE ranking from Section III-A, confirming that modeling accuracy propagates into detection performance. BOKPCA's intermediate position is consistent with its intermediate MSE: competitive with BONN at low noise but less reliable under high noise. The MMGLR chart outperforms the Q chart across all models, with average DRs of 69% versus 47.9% at FAR $\approx 1\%$, and interval data reduces average $\hat{e}$ from 36.1 (scalar) to 20.8 (interval). In the TEP case study, PCA and BONN perform nearly equivalently ($\hat{e}$ of 10.1 and 9.4), consistent with the prediction plots in Section III-A which showed all models fitting the TEP data similarly. This indicates that data abundance may sometimes compensate for PCA's linear limitation. On the other hand, in the GTL reactor data, the modeling gap identified in Section III-A carries through fully into fault detection: BONN achieves $\hat{e} = 8.8$ versus 18.3 for PCA, a reduction of over 50%. Fault 2 (thermal runaway) is the most discriminating, with DRs of 29.4% and 75.9% for PCA and BONN respectively at FAR $\approx 1\%$. This 46.5% point gap is directly traceable to PCA's inability to capture the nonlinear thermal coupling dynamics visible in Figure 6 [7], [1].

TABLE II: Cross-case summary: average $\hat{e}$ values using MMGLR with interval data. BOKPCA is evaluated on synthetic data only; see text for rationale.

Model	Synthetic	TEP	GTL
PCA	31.6	10.1	18.3
BOKPCA	27.9	—	—
BONN	25.8	9.4	8.8
Δ (PCA $-$ BONN)	5.8	0.7	9.5

IV. CONCLUSION

This paper presented a two-stage comparative analysis of PCA, BOKPCA, and BONN, evaluating prediction accuracy against noise-free ground truth and assessing how modeling differences propagate into fault detection performance. From a practical standpoint, PCA remains the least computationally demanding of the three methods, while BONN incurs the highest cost due to Bayesian hyperparameter optimization and backpropagation-based training; BOKPCA falls between the two, with cost driven primarily by kernel matrix computation and the pre-image estimation step. On the modeling side, the synthetic MSE analysis showed that BONN consistently achieves the lowest prediction error across noise levels, with a minimum MSE of 0.056 at SNR = 5 and 0.008 at SNR = 50, outperforming PCA (0.074 and 0.017 respectively) in both cases. BOKPCA reaches accuracy equivalent to BONN at low noise (0.008) but degrades substantially at high noise due to the higher sensitivity of its feature-space model selection criterion to noise contamination: the scree-plot-based selection used for PCA and BONN estimated the correct optimal dimensionality at both noise levels, while BOKPCA's cross-validation MSE plot overestimated it as $\hat{r} = 11$ against the true optimum $r^* = 5$ at SNR = 5. For the TEP, prediction plots confirmed that all three models perform comparably due to the dataset's high noise level. For the GTL reactor, the nonlinear models, particularly BONN, visibly outperformed PCA in capturing the process dynamics, with PCA exhibiting spurious oscillations and divergence in nonlinear transition regions where BONN remained tightly aligned with the measured data.

These modeling differences carry directly into fault detection. The detection ranking on the synthetic dataset (BONN $>$ BOKPCA $>$ PCA) mirrors the MSE ranking exactly, confirming that prediction accuracy is the primary driver of detection sensitivity. On the TEP, where all models produce similar predictions, PCA and BONN perform nearly equivalently ($\Delta\hat{e} = 0.7$). On the GTL reactor, where the

modeling gap is largest, the detection gap is also largest ($\Delta\hat{e} = 9.5$, a 52% reduction in $\hat{e}$ for BONN relative to PCA). The MMGLR chart and interval data analysis provide further orthogonal improvements across all model and process combinations, consistent with prior work [7], [1]. Future work will extend this analysis to the fault classification stage, where residual quality similarly governs classifier performance.

ACKNOWLEDGMENTS

The statements herein are solely the responsibility of the authors.

REFERENCES

[1] M. N. Nounou, H. N. Nounou, N. Basha, and B. Malluhi, *Advances in Data-Driven Modeling, Fault Detection, and Fault Identification: Applications to Chemical Processes*, 1st ed. Elsevier, 2026. [Online]. Available: https://shop.elsevier.com/books/advances-in-data-driven-modeling-fault-detection-and-fault-identification/nounou/978-0-443-33482-5

[2] I. T. Jolliffe and J. Cadima, "Principal component analysis: a review and recent developments," *Philosophical Transactions of the Royal Society A: Mathematical, Physical and Engineering Sciences*, vol. 374, 2016.

[3] T. Kurita, "Principal component analysis (pca)," *Computer Vision: A Reference Guide*, pp. 1–4, 2019.

[4] R. Fezai, B. Malluhi, N. Basha, G. Ibrahim, H. A. Choudhury, M. S. Challiwala, H. Nounou, N. Elbashir, and M. Nounou, "Bayesian optimization of multiscale kernel principal component analysis and its application to model gas-to-liquid (gtl) process data," *Energy*, vol. 284, p. 129221, 2023. [Online]. Available: https://www.sciencedirect.com/science/article/pii/S0360544223026154

[5] N. Basha, G. Ibrahim, H. A. Choudhury, M. S. Challiwala, R. Fezai, B. Malluhi, H. Nounou, N. Elbashir, and M. Nounou, "Bayesian-optimized neural networks and their application to model gas-to-liquid plants," *Gas Science and Engineering*, vol. 113, p. 204964, 2023.

[6] N. Basha, "Advanced data-driven process monitoring framework and its application to chemical processes," Doctor of Philosophy Dissertation, Department of Chemical Engineering, Texas A&M University, 2024.

[7] N. Basha, R. Fezai, B. Malluhi, K. Dhibi, G. Ibrahim, H. A. Choudhury, M. S. Challiwala, H. Nounou, N. Elbashir, and M. Nounou, "Advanced data-driven fault detection in gas-to-liquid plants," *Computers & Chemical Engineering*, p. 109098, 2025. [Online]. Available: https://www.sciencedirect.com/science/article/pii/S0098135425001024

[8] M. R. Reynolds-Jr. and J. Lou, "An evaluation of a glr control chart for monitoring the process mean," *Journal of Quality Technology*, vol. 42, pp. 287–310, 2010.

[9] M. Z. Sheriff, N. Basha, M. N. Karim, H. Nounou, and M. Nounou, "Fault detection of single and interval valued data using statistical process monitoring techniques," in *Fault Detection, Diagnosis and Prognosis*. IntechOpen London, UK, 2019, p. 105.

[10] N. Basha, M. Z. Sheriff, C. Kravaris, H. Nounou, and M. Nounou, "Multiclass data classification using fault detection-based techniques," *Computers & Chemical Engineering*, vol. 136, p. 106786, 2020.

[11] W. H. Woodall and M. A. Mahmoud, "The inertial properties of quality control charts," *Technometrics*, vol. 47, no. 4, pp. 425–436, 2005.